ChemPubSoc Europe
DOI: 10.1002/cmdc.201402453
CHEMMEDCHEM Full Papers

Optimization of 1,2,5-Thiadiazole Carbamates as Potent and Selective ABHD6 Inhibitors

Jayendra Z. Patel,*[a] Tapio J. Nevalainen,[a] Juha R. Savinainen,[b] Yahaya Adams,[a] Tuomo Laitinen,[a] Robert S. Runyon,[c] Miia Vaara,[b] Stephen Ahenkorah,[a] Agnieszka A. Kaczor,[a, d] Dina Navia-Paldanius,[b] Mikko Gynther,[a] Niina Aaltonen,[a] Amit A. Joharapurkar,[e] Mukul R. Jain,[e] Abigail S. Haka,[c] Frederick R. Maxfield,[c] Jarmo T. Laitinen,[b] and Teija Parkkari*[a]

Dedicated to Dr. Saurin Raval, principal scientist at Zydus Research Centre, India.

At present, inhibitors of α/β-hydrolase domain 6 (ABHD6) are viewed as a promising approach to treat inflammation and metabolic disorders. This article describes the development of 1,2,5-thiadiazole carbamates as ABHD6 inhibitors. Altogether, 34 compounds were synthesized, and their inhibitory activity was tested using lysates of HEK293 cells transiently expressing human ABHD6 (hABHD6). Among the compound series, 4-morpholino-1,2,5-thiadiazol-3-yl cyclooctyl(methyl)carbamate (JZP-430) potently and irreversibly inhibited hABHD6 (IC_{50} = 44 nM) and showed ~230-fold selectivity over fatty acid amide hydrolase (FAAH) and lysosomal acid lipase (LAL), the main off-targets of related compounds. Additionally, activity-based protein profiling indicated that JZP-430 displays good selectivity among the serine hydrolases of the mouse brain membrane proteome. JZP-430 has been identified as a highly selective, irreversible inhibitor of hABHD6, which may provide a novel approach in the treatment of obesity and type II diabetes.

Introduction

In the central nervous system (CNS), the α/β hydrolase domain containing 6 (ABHD6), an integral membrane serine hydrolase, contributes to a small portion of the in vivo degradation of 2-arachidonoylglycerol (2-AG), an endogenous lipid signaling molecule activating the cannabinoid receptors.[1] In the brain, ABHD6 along with the serine hydrolases monoacylglycerol lipase (MAGL) and α/β hydrolase domain containing 12 (ABHD12) account for ~98% of 2-AG degradation;[2] 85% of 2-AG is metabolized by MAGL and 9% by ABHD12 while only 4% is attributed to ABHD6.[2] The remaining ~2% is hydrolyzed by additional enzymes, including fatty acid amide hydrolase (FAAH). MAGL, ABHD12 and ABHD6 have different tissue distribution and subcellular localization, suggesting that they may have distinct roles in controlling the lifetime of 2-AG.[1] To distinguish between these roles and to gain in-depth understanding of their physiological significance, selective ABHD6 inhibitors are needed.

Recent reports have suggested ABHD6 as an emerging therapeutic target for the treatment of inflammation, metabolic disorders (obesity and type II diabetes mellitus) and epilepsy.[3–6] ABHD6 inhibitors may have certain advantages over inhibitors of MAGL and ABHD12. First, genetic inactivation of MAGL causes a massive increase in brain 2-AG levels, leading to psychotropic side effects and cannabinoid receptor desensitization.[7–9] Second, even though ABHD12 is still poorly characterized, studies with genetically ABHD12 deficient mice suggest that inactivation of this serine hydrolase leads to age-dependent symptoms that resemble the human neurodegenerative disorder PHARC (polyneuropathy, hearing loss, ataxia, retinosis pigmentosa, cataract).[10] Inhibition of ABHD6, on the other hand, is expected to induce only a slight increase in 2-AG levels suggesting that ABHD6 inhibitors may have less CNS-related side effects.[2,4,11]

To date, only a few ABHD6 inhibitors have been reported (Figure 1). In 2007, Cravatt and co-workers reported the identification of WWL70 (**1**), a potent and selective carbamate-

[a] *J. Z. Patel, Dr. T. J. Nevalainen, Y. Adams, Dr. T. Laitinen, S. Ahenkorah, Dr. A. A. Kaczor, Dr. M. Gynther, N. Aaltonen, Dr. T. Parkkari*
School of Pharmacy, University of Eastern Finland
P.O. Box 1627, 70211 Kuopio (Finland)
E-mail: jayendra.patel@uef.fi
teija.parkkari@uef.fi

[b] *Dr. J. R. Savinainen, M. Vaara, D. Navia-Paldanius, Dr. J. T. Laitinen*
School of Medicine, Institute of Biomedicine/Physiology
University of Eastern Finland
P.O. Box 1627, 70211 Kuopio (Finland)

[c] *R. S. Runyon, Dr. A. S. Haka, Prof. F. R. Maxfield*
Department of Biochemistry, Weill Cornell Medical College
1300 York Avenue, New York, NY 10065 (USA)

[d] *Dr. A. A. Kaczor*
Department of Synthesis & Chemical Technology of Pharmaceutical Substances, Faculty of Pharmacy with Division of Medical Analytics
Medical University of Lublin, 4a Chodzki St., 20093 Lublin (Poland)

[e] *Dr. A. A. Joharapurkar, Dr. M. R. Jain*
Department of Pharmacology & Toxicology, Zydus Research Centre
Sarkhej Bavla NH8A, Moraiya, Ahmedabad 382210, Gujarat (India)

Supporting information for this article is available on the WWW under http://dx.doi.org/10.1002/cmdc.201402453.

© 0000 Wiley-VCH Verlag GmbH & Co. KGaA, Weinheim

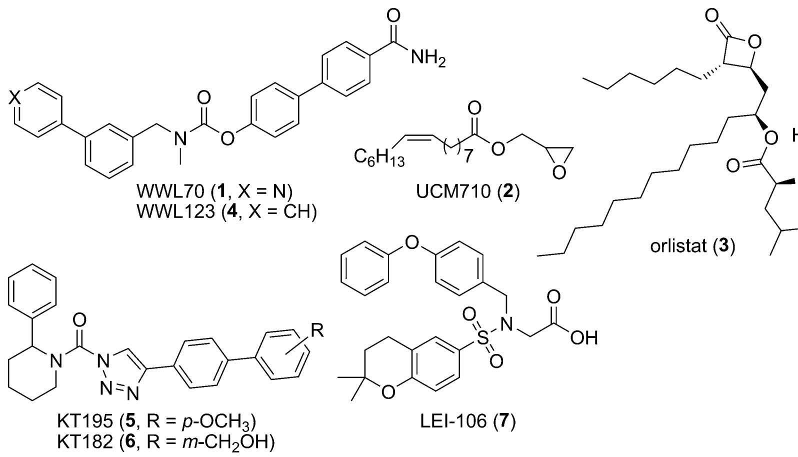

Figure 1. Selective and non-selective ABHD6 inhibitors (**1**–**7**).

based inhibitor whose selectivity among the serine hydrolases was evaluated using activity-based protein profiling (ABPP).[12] Marrs et al. described UCM710 (**2**), a dual inhibitor of ABHD6 and FAAH.[13] Examples of non-selective ABHD6 inhibitors include methylarachidonoyl fluorophosphonate (MAFP), orlistat (tetrahydrolipstatin, THL, **3**), RHC-80267, and the triterpene pristimerin.[14] Recently, Cravatt and colleagues disclosed several other ABHD6 inhibitors such as carbamate based compound WWL123 (**4**), an isostere analogue of WWL70, and triazole urea analogues (e.g., KT195 (**5**) and KT182 (**6**)) as potent and selective ABHD6 inhibitors.[15–17] Very recently, Janssen et al. reported glycine sulfonamide analogue LEI-106 (**7**) as a potent and selective dual inhibitor of sn-1-diacylglycerol lipase α (DAGL-α) and ABHD6.[18]

In 2010, Helquist and co-workers reported 1,2,5-thiadiazole carbamates (**I**, Figure 2) as potent inhibitors of lysosomal acid lipase (LAL, also known as LIPA).[19] LAL was recently identified as a potential therapeutic target for Niemann–Pick disease type C (NPC), a condition characterized by a gradual lysosomal accumulation of lipids such as cholesteryl esters and triglycerides. Additionally, Helquist and colleagues reported that orlistat (**3**), which acts as a broad-spectrum lipase inhibitor, also inhibits LAL. So far, numerous carbamate compounds have been reported as inhibitors of endocannabinoid metabolizing enzymes,[12,15,20–23] (for recent reviews, see References [24–27]). We therefore thought to use 1,2,5-thiadiazole carbamate (**I**, Figure 2) scaffold for the development of inhibitors of the endocannabinoid metabolizing enzymes. A limited structure-activity relationship (SAR) study based on this scaffold has been reported,[19] thus leaving room for further optimization of the 1,2,5-thiadiazole carbamate scaffold (**II**, Figure 2). The mechanism for LAL inhibition via 1,2,5-thiadiazole carbamates is suggested to occur by carbamoylation of the active site serine with the 1,2,5-thiadiazole alcohol group serving as the leaving group (I, Figure 2). In our compound series (Figure 2 and 3), we used 1,2,5-thiadiazole scaffold by introducing different cyclic and non-cyclic secondary amines at the main core while a small set of different cyclic amines were introduced as potential leaving groups.

Herein we report the optimization of 1,2,5-thiadiazole carbamates as novel ABHD6 inhibitors. The selectivity against other endocannabinoid targets, serine hydrolases of the mouse membrane proteome as well as LAL has been evaluated, and the inhibitory activity data have been used to explore the SAR. Finally, homology modeling and molecular docking were used in attempts to provide insight into how the best compounds interacted optimally with the active site of ABHD6.

Results and Discussion

Chemistry

The synthesis of 1,2,5-thiadiazole carbamates (**22**–**55**) is shown in Scheme 1. Commercially available 3,4-dichloro-1,2,5-thiadiazole was coupled with the appropriate secondary amine to afford a corresponding monochloro 1,2,5-thiadiazole derivative (**8**–**14**), which was then converted in to 1,2,5-thiadiazole alcohol (**15**–**21**) via treatment with aqueous alkali. Finally, coupling with appropriate carbamoyl chloride gave the desired 1,2,5-thiadiazole carbamates (**22**–**55**). The synthesis of monochloro 1,2,5-thiadiazole derivatives (**8**–**14**), 1,2,5-thiadiazole alcohol derivatives (**15**–**21**) and carbamoyl

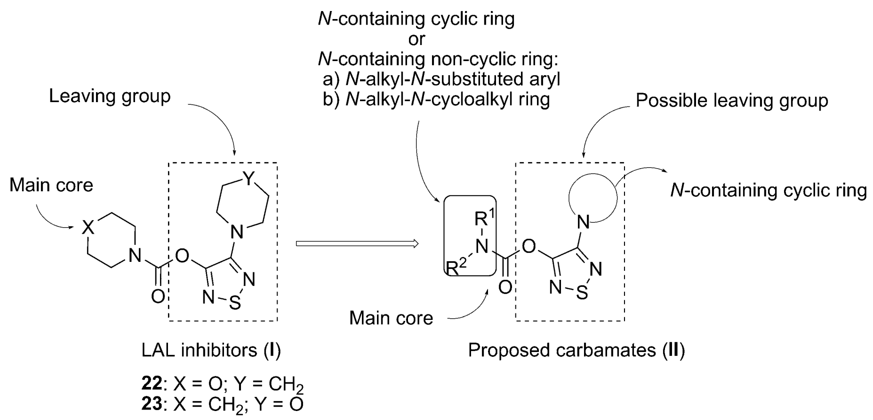

Figure 2. Optimization of 1,2,5-thiadiazole carbamates.

© 0000 Wiley-VCH Verlag GmbH & Co. KGaA, Weinheim

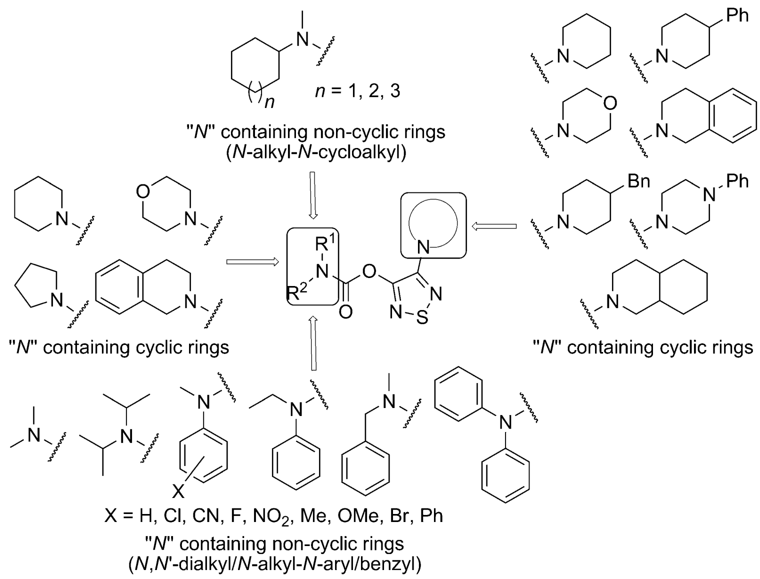

Figure 3. Variations around the 1,2,5-thiadiazole scaffold.

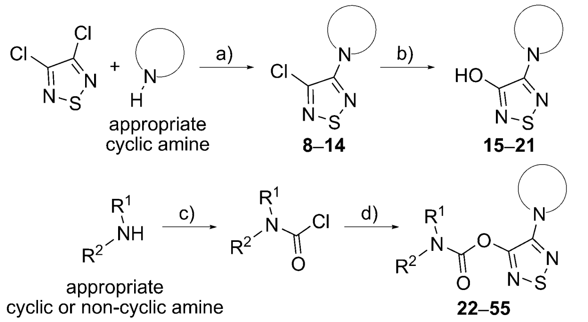

Scheme 1. Synthesis of 1,2,5-thiadiazole carbamate derivatives **22**–**55**. *Reagents and conditions*: a) 110–120 °C, 2–6 h or K_2CO_3, DMF, 100–110 °C, 6–10 h; b) aq. NaOH or KOH, DMSO, reflux, 1–6 h; c) pyridine, CH_2Cl_2, triphosgene, 0–5 °C or −78 °C, 3–4 h; d) dry THF, **15**–**21**, KO*t*Bu, 0–25 °C, 16–24 h.

chloride compounds was performed as per literature procedures with minor modifications (see Supporting Information).

SAR of ABHD6 inhibitors

The inhibitory activities of the synthesized compounds were initially screened at 1 μM concentration against hABHD6 and hABHD12, and at 10 μM concentration against hFAAH and hMAGL. As FAAH was found to be the main off-target site, inhibitory activity data concerning hABHD6 and hFAAH are presented in Tables 1–4, while results of the hABHD12 and hMAGL inhibition experiments are presented in Tables S3 and S4 (see Supporting Information).

Cyclic "N" containing thiadiazole carbamates (structural modifications of main core and leaving group)

As an initial step, we synthesized two previously reported LAL inhibitors having piperidine and morpholine rings at opposite sides of the thiadiazole core, that is, compounds **22** and **23** (Table 1). Both **22** and **23** showed excellent ABHD6 inhibitory activities with potencies in the low nanomolar range (IC_{50} 52 nM and 85 nM, respectively) but these compounds inhibited also FAAH with moderate potencies (IC_{50} 0.40 and 0.30 μM, respectively). As compound **22** was more potent of these two we retained the thiadiazole piperidine core in the newly synthesized analogues **24** and **25**. We found a similar inhibitory activity trend for pyrrolidine analogue **24** and 1,2,3,4-tetrahydroisoquinoline analogue **25**, although decreased inhibitory potencies toward ABHD6 and FAAH were observed. Because none of the analogues showed significant improvement in selectivity, we clarified the effect of the leaving group by synthesizing different thiadiazole carbamates (**26**–**30**) in which the piperidine carbamate scaffold was kept intact. Substituted piperidine analogues **26** and **28** as well as piperazine analogue of **26** (compound **27**) showed similar FAAH inhibition, while only weak inhibition of ABHD6 was observed. However, fused bicyclic analogues (compounds **29** and **30**) showed improved FAAH inhibition (IC_{50} 17 nM and 31 nM, respectively) while moderate inhibitory activities were observed against ABHD6 (IC_{50} 0.46 and 0.56 μM, respectively). Compounds **22**–**30** did not show any appreciable inhibition of hMAGL or hABHD12 (Table S3, Supporting Information).

To reveal additional off-targets, we screened selected analogues (**22**, **23**, **29** and **30**) at 1 μM concentration against the serine hydrolases of the mouse brain membrane proteome using competitive ABPP, essentially as previously described[14,28] (Figure S1, Supporting Information). We found that all the tested compounds showed complete inhibition of FAAH, and inhibition of ABHD6 was also evident. Moreover, an unidentified serine hydrolase (a protein band migrating at ~30 kDa) was found as an off-target site of the four analogues.

Non-cyclic "N" containing thiadiazole carbamates (structural modifications of the main core)

As no satisfactory selectivity for ABHD6 over FAAH was achieved with the analogues **22**–**30** (selectivity ratio < 30-fold), we explored the thiadiazole carbamates further by opening the "N" containing ring system in the main core (see Figure 2). *N*,*N*-dimethyl analogue **31** showed weak FAAH inhibition (IC_{50}

© 0000 Wiley-VCH Verlag GmbH & Co. KGaA, Weinheim

Table 1. Inhibitory activities of 1,2,5-thiadiazole carbamates **22**–**30** against hABHD6 and hFAAH.

Compd	Structure	pIC_{50} (range)[a][b] hABHD6	hFAAH
22	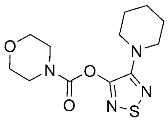	7.28 (7.23–7.32) [0.052]	6.39 (6.29–6.49) [0.40]
23	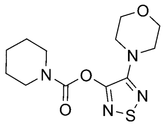	7.07 (7.03–7.10) [0.085]	6.48 (6.41–6.55) [0.30]
24	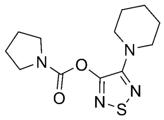	6.58 (6.43–6.73) [0.26]	6.09 (6.01–6.18) [0.81]
25	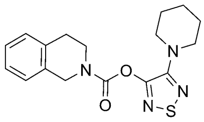	6.88 (6.80–6.95) [0.13]	6.25 (6.23–6.27) [0.56]
26	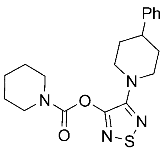	41 %[b]	5.83 (5.34–6.31) [1.47]
27	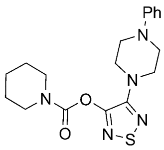	40 %[b]	6.68 (6.51–6.84) [0.21]
28	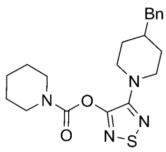	15 %[b]	6.49 (6.30–6.67) [0.32]
29	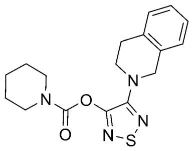	6.34 (6.22–6.45) [0.46]	7.77 (7.71–7.83) [0.017]
30	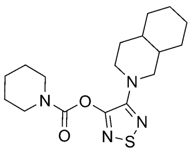	6.25 (6.19–6.31) [0.56]	7.51 (7.48–7.53) [0.031]
WWL70 (**1**)	–	7.07 ± 0.05 [0.085][c]	30 %[b]
THL (**3**)	–	7.32 ± 0.11 [0.048][c]	NA[d]
JZP-327A[e]	–	NI[d]	7.94 (7.91–7.97) [0.011]

[a] pIC_{50} values ($-\log_{10}$[IC_{50}, μм]) represent the mean (range) of two independent experiments performed in duplicate. IC_{50} values were calculated for those compounds exhibiting ≥50 % inhibition at 1 μм for hABHD6 and at 10 μм for hFAAH; where <50 % inhibition was observed, the percent inhibition at the aforementioned concentration is given. IC_{50} values are derived from the mean pIC_{50} values as shown in parentheses. [b] Percent inhibition values represent the mean of two independent experiments performed in duplicate. [c] pIC_{50} values are the mean ±SEM of three independent experiments performed in duplicate; data taken from Ref. [14]. [d] NA: not analyzed; NI: no inhibition. [e] *S*-3-(1-(4-isobutylphenyl)ethyl)-5-methoxy-1,3,4-oxadiazol-2(3*H*)-one (JZP-327A)[29] was used as reference FAAH inhibitor.

6.45 μм) while no inhibition was observed against the other tested enzymes (Table 2 and Tables S3,S4 in Supporting Information). Replacing one methyl group of **31** with a phenyl group (compound **32**) resulted in excellent ABHD6 inhibitory activity (IC_{50} 22 nм), and also improved ABHD6 selectivity (404-fold) over FAAH (IC_{50} 8.9 μм). However, adding another phenyl group in the compound **32** (compound **33**) resulted in complete loss of activity toward all the tested enzymes. Additionally, the *N*,*N*-diisopropyl analogue (compound **34**) showed loss of activity, which may be due to shielding of the carbonyl group from attack by the serine hydroxy group at the active site of the enzyme. As compound **32** turned out to be the best ABHD6 inhibitor, we investigated further the optimal structural requirement needed for inhibitory activity and selectivity. Changing the methyl group of compound **32** into an ethyl (compound **35**) resulted in a ~20-fold drop in potency, while changing the phenyl (**32**) into benzyl (**36**) resulted in a 2-fold increase in ABHD6 inhibitory activity (IC_{50} 10 nм). Compound **35** showed no noticeable inhibition of the other tested enzymes (Table 2 and Table S3 in Supporting Information), while loss of selectivity was observed for compound **36** as it also showed improved FAAH inhibition (IC_{50} 67 nм) as well as weak MAGL inhibition (IC_{50} 5.6 μм; Table S3, Supporting Information).

In competitive ABPP of the mouse brain membrane proteome, compounds **32** and **36** were found to inhibit ABHD6 completely (Figure S2, Supporting Information) at 1 μм concentration. As expected, **36** also targeted FAAH. In addition, an unidentified serine hydrolase (a protein band migrating at ~30 kDa) was inhibited by **32**.

© 0000 Wiley-VCH Verlag GmbH & Co. KGaA, Weinheim

Table 2. Inhibitory activities of novel 1,2,5-thiadiazole carbamates **31**–**36** against ABHD6 and FAAH.

Compd	Structure	pIC_{50}[a] hABHD6	pIC_{50}[a] hFAAH
31	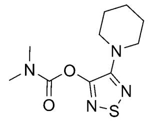	10%[b]	5.19 (5.17–5.20) [6.45]
32	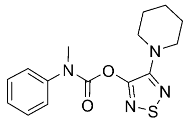	7.66 ± 0.07 [0.022]	5.06 (5.05–5.07) [8.91]
33	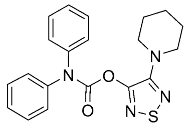	NI[c]	NI[c]
34	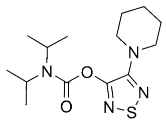	NI[c]	NI[c]
35	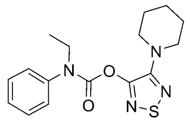	6.33 ± 0.13 [0.47]	24%[b]
36	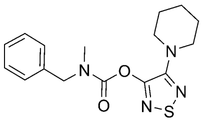	8.01 ± 0.03 [0.010]	7.20 (7.17–7.23) [0.063]

[a] pIC_{50} values ($-\log_{10}[IC_{50}$, μM]) represent the mean ± SEM of three independent experiments performed in duplicate (for hABHD6) or the mean (range) of two independent experiments performed in duplicate (for hFAAH). IC_{50} values were calculated for those compounds exhibiting ≥50% inhibition at 1 μM for hABHD6 and at 10 μM for hFAAH; where <50% inhibition was observed, the percent inhibition at the aforementioned concentration is given. IC_{50} values are derived from the mean pIC_{50} values as shown in parentheses. [b] Percent inhibition values represent the mean of two independent experiments performed in duplicate. [c] NI: no inhibition.

N-Methyl-*N*-substituted phenyl thiadiazole carbamates

Next, we investigated the effect of different substituents on the phenyl ring of compound **32** by synthesizing the analogues **37**–**51** (Table 3). Among these, compounds having an electron withdrawing group (EWG) at the *para* position of the phenyl ring (compounds **37**, **41** and **42**) showed a 4- to 55-fold loss of ABHD6 inhibitory activity, and the cyano analogue **40** showed complete loss of activity. Switching the *para*-nitro substituent (compound **37**) to the *meta* position (compound **38**) retained activity, while in the *ortho* position (compound **39**) ABHD6 inhibitory activity was completely lost. Furthermore, both *para*- and *meta*-fluoro analogues (compounds **42** and **43**) were almost equipotent in inhibiting ABHD6. In a similar fashion, electron donating groups (EDG) at the *para*-position resulted in a 6- to 12-fold loss of ABHD6 inhibitory activity, depending on the nature of EDG (**44** and **47**). However, switching back the methyl substituent from the *para* (**44**) to the *meta* position (**45**) showed almost a threefold improvement in ABHD6 inhibition, while methoxy analogues (compounds **47** and **48**) showed only marginal differences in their ABHD6 inhibitory activities. However, their *ortho* analogues (**46** and **49**) showed complete loss of ABHD6 inhibition. Finally, substitution of the phenyl ring with the *meta*-phenyl resulted in almost a 40-fold loss (compound **50**) of ABHD6 inhibitory potency, and the bulky trimethyl substitution (compound **51**) lead to complete loss of activity. None of the analogues **37**–**51** showed appreciable inhibition of hFAAH, hMAGL or hABHD12 (Table 3 and Table S4 in Supporting Information).

To screen inhibitor selectivity among the serine hydrolases in mouse brain membrane proteome, we performed competitive ABPP for selected analogues (**42** and **45**) and found complete inhibition of ABHD6 at 1 μM concentration (Figure S3, Supporting Information). In addition, an unidentified serine hydrolase migrating at ~30 kDa was targeted by the compounds **42** and **45**.

N-Methyl-*N*-cycloalkyl thiadiazole carbamates

As no further improvement in ABHD6 inhibitory activity or selectivity was obtained with the analogues **37**–**51**, we replaced the phenyl ring of compound **32** by different cycloalkyl rings (compounds **52**–**55**, Table 4). Increasing the size of the cycloalkyl ring from a six- to eight-membered ring (**52**–**54**) resulted in an approximate 2–4-fold loss of ABHD6 inhibition, while no inhibition of FAAH was observed at 10 μM. As increased ring size also causes increased lipophilicity (i.e., clog*P* for **52** is 4.4 while for **54** it is 5.5; Table S5, Supporting Information), we replaced the piperidine ring of compound **54** with a morpholine ring (compound **55**). Consequently, compound **55** had ABHD6 inhibitory activity similar to that of compounds **52** and **53**, while being less lipophilic (clog*P* = 4.1). None of these compounds **52**–**55** showed any inhibition of the other enzymes tested (Table S4, Supporting Information). Finally, when these analogues (**52**–**55**) were tested using competitive ABPP, all the compounds except compound **52** selectively targeted ABHD6 when tested at 1 μM concentration (Figure S4, Supporting Information). Compound **52** additionally targeted the ~30 kDa serine hydrolase with unknown identity.

ABHD6 selectivity

LAL inhibitory activity

As our compound series was developed from the compounds that were originally designed as LAL inhibitors, we tested the activity of these compounds toward LAL, essentially as previously described.[19] We selected several potent analogues (**22**, **23**, **29**, **30**, **32**, **36**, **42**, **45** and **52**–**55**) from our compound series containing both known LAL inhibitors as well as novel

© 0000 Wiley-VCH Verlag GmbH & Co. KGaA, Weinheim

Table 3. Inhibitory activities of novel 1,2,5-thiadiazole carbamates **37–51** against ABHD6 and FAAH.

Compd	Structure	pIC_{50}[a] hABHD6	Inhib. [%][b] hFAAH
37	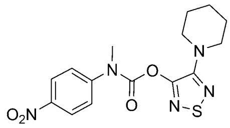	5.90 ± 0.08 [1.25]	19
38	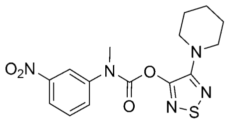	5.92 ± 0.05 [1.20]	11
39	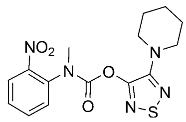	NI[c]	46
40	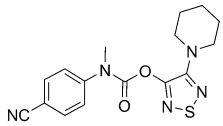	15 %[b]	19
41	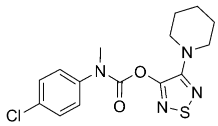	6.39 ± 0.03 [0.41]	16
42	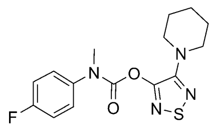	7.11 ± 0.07 [0.078]	22
43	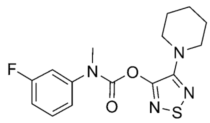	7.22 ± 0.05 [0.060]	48
44	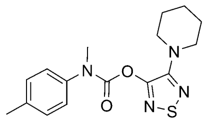	6.83 ± 0.04 [0.15]	21
45	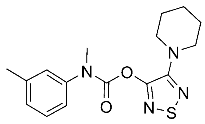	7.27 ± 0.07 [0.054]	9
46	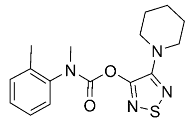	17 %[b]	40
47	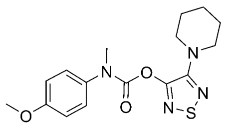	6.58 ± 0.04 [0.26]	17
48	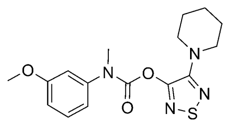	6.71 ± 0.07 [0.19]	17
49	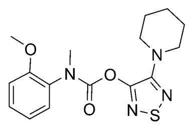	11 %[b]	18
50	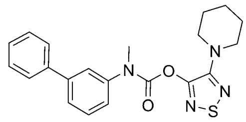	6.04 ± 0.10 [0.91]	13
51	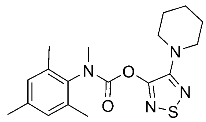	NI[c]	7

[a] pIC_{50} values ($-\log_{10}$ [IC_{50}, μM]) represent the mean ± SEM of three independent experiments performed in duplicate. IC_{50} values were calculated for those compounds exhibiting ≥ 50 % inhibition at 1 μM and are derived from the mean pIC_{50} values as shown in parentheses. [b] Percent inhibition at 1 μM for hABHD6 and at 10 μM for hFAAH is reported; values represent the mean of two independent experiments performed in duplicate. [c] NI: no inhibition.

Table 4. Inhibitory activities of novel 1,2,5-thiadiazole carbamates **52–55** against ABHD6 and FAAH.

Compd	Structure	pIC_{50}[a] hABHD6	Inhib. [%][b] hFAAH
52	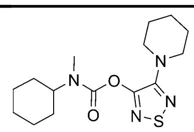	7.36 ± 0.05 [0.044]	16
53	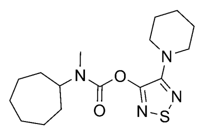	7.37 ± 0.05 [0.043]	21
54	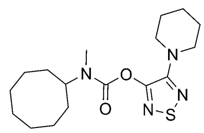	7.14 ± 0.06 [0.072]	13
JZP-430 (**55**)	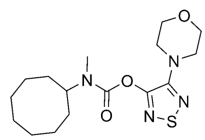	7.36 ± 0.05 [0.044]	18

[a] pIC_{50} values ($-\log_{10}$ [IC_{50}, μM]) represent the mean ± SEM of three independent experiments performed in duplicate. IC_{50} values were calculated for those compounds exhibiting ≥ 50 % inhibition at 1 μM and are derived from the mean pIC_{50} values as shown in parentheses. [b] Percent inhibition at 10 μM; values represent the mean of two independent experiments performed in duplicate.

ABHD6 inhibitors, and tested them at 10 μM concentration. (Figure 4). Among the cyclic analogues (**22**, **23**, **29** and **30**) the previously reported LAL inhibitors **22** and **23** were found to inhibit LAL activity almost completely. A similar trend was observed for our compounds **29** and **30**, both having bulky cyclic rings as potential leaving groups. Among the non-cyclic analogues (**32**, **36**, **42**, **45** and **52–55**), *N*-methyl-*N*-aryl analogues **32**, **42** and **45** were found to inhibit LAL activity by 25–35 %,

© 0000 Wiley-VCH Verlag GmbH & Co. KGaA, Weinheim

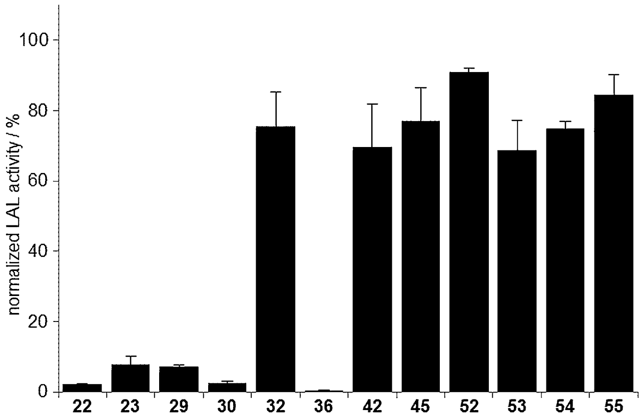

Figure 4. Lysosomal acid lipase (phLAL) activity in the presence of selected thiadiazole carbamates, each at 10 μM. Enzymatic activity at 37 °C was quantified as background-corrected 4-methylumbelliferone fluorescence, normalized to the DMSO control average value. Data are averages ± SEM from two independent experiments ($n=5$ wells used for quantification per experiment).

and interestingly, *N*-methyl-*N*-benzyl analogue **36** showed > 99 % inhibition. *N*-methyl-*N*-cycloalkyl analogues **52**–**55** were also weak LAL inhibitors showing < 33 % inhibition at 10 μM concentration. Notably, the ABHD6 inhibitor **55** (JZP-430) was found to have only a slight inhibition (< 20 %) of LAL at 10 μM concentration. We determined the dose–response curves and calculated the IC_{50} values for those compounds that in the initial screen showed > 50 % inhibition (Table S6, Supporting Information).

Activity-based protein profiling (ABPP)

Next, we tested in more detail the selectivity of our carbamate-based analogue JZP-430 (**55**) using competitive ABPP of the mouse brain membrane proteome (Figure 5). We used earlier reported inhibitors WWL70 (**1**)[12] and JZP-327A[29] at the indicated concentrations to locate the bands of ABHD6 and FAAH, respectively. We found that JZP-430 (**55**) inhibited ABHD6 dose-dependently, being effective already at 0.25 μM concentration. Selective inhibition of ABHD6 was detected even at 1 μM concentration while negligible inhibition of FAAH was observed at 2.5 μM concentration. At 20-fold (5 μM) concentration partial inhibition of FAAH was detected. In short, when tested at below 2.5 μM concentration, JZP-430 (**55**) appeared to be selective for ABHD6 over the other detectable brain serine hydrolases, including FAAH, MAGL and ABHD12.

Selectivity over the other endocannabinoid targets

Finally, JZP-430 (**55**) was tested against the cannabinoid CB_1 and CB_2 receptors but it did not show any appreciable agonist or antagonist activity when tested at 10 μM concentration (Table S7, Supporting Information).

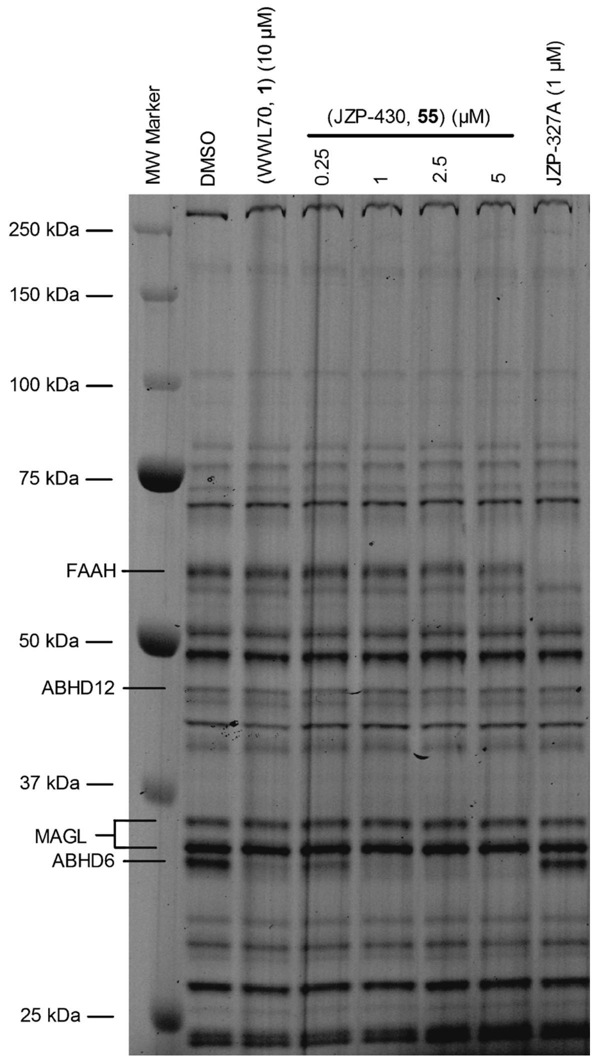

Figure 5. Competitive ABPP of compound **55** (JZP-430) among the serine hydrolases in mouse whole-brain membrane proteome. Molecular weight markers are indicated at left. Reference inhibitors WWL70 (**1**) and JZP-327A were used at the indicated concentrations to identify the following serine hydrolases from the gel: ABHD6, inhibited by WWL70 (**1**)[12] and FAAH, inhibited by JZP-327A.[29] In addition, protein bands corresponding to MAGL (doublet) and ABHD12 are indicated. Note that JZP-430 (**55**) inhibits only probe labeling of ABHD6 at 0.25 μM. Selective inhibition of ABHD6 was evident at concentrations < 2.5 μM, whereas partial inhibition of FAAH was observed at 5 μM (20-fold). The gel is representative of two ABPP experiments with similar outcomes.

Reversibility of ABHD6 inhibition

To get deeper insight into ABHD6 binding mode of JZP-430 (**55**), we tested its potency to inhibit ABHD6 using a 96-well format dilution method.[28] As a result, both the established irreversible ABHD6 inhibitor WWL70 (**1**) and JZP-430 (**55**) fully retained their potencies during the 90 min incubation period following a fast 40-fold dilution of the enzyme-inhibitor complex (Figure 6), a finding suggesting that compound **55** inactivated hABHD6 in an irreversible manner.

© 0000 Wiley-VCH Verlag GmbH & Co. KGaA, Weinheim
These are not the final page numbers! ↗↗

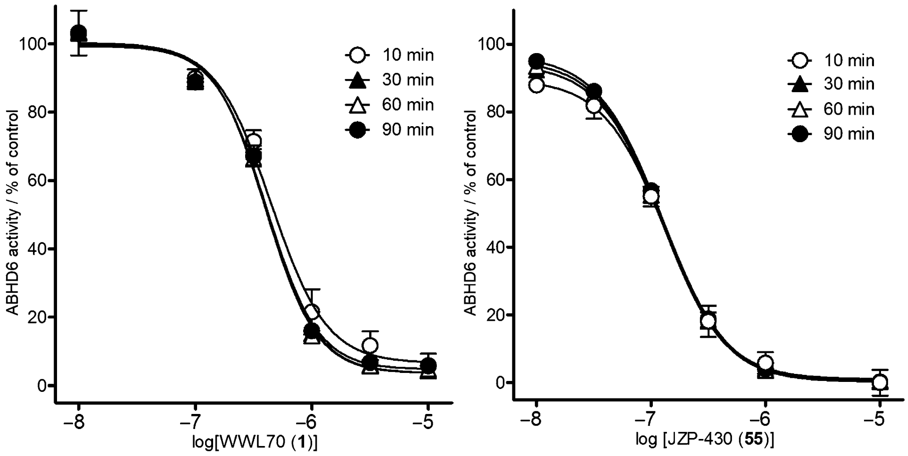

incubation time [min]	pIC50 ± SEM	
	WWL70 (**1**)	JZP-430 (**55**)
10	6.35 ± 0.07	6.88 ± 0.05
30	6.39 ± 0.03	6.90 ± 0.02
60	6.40 ± 0.03	6.91 ± 0.02
90	6.40 ± 0.03	6.90 ± 0.02

Figure 6. Potencies (pIC_{50}) of the irreversible ABHD6 inhibitor WWL70 (**1**) and compound **55** (JZP-430) are not time-dependently changed following a rapid 40-fold dilution of inhibitor-treated hABHD6 preparation, indicating that within the timeframe studied, compound **55** acts as an irreversible ABHD6 inhibitor. Note that due to methodological limitations, the IC_{50} values obtained by the dilution method are not directly comparable to those obtained using the routine assay protocol (Table 4).[28,30] Data are mean ±SEM from three independent experiments (each with duplicate wells).

Molecular modeling

We assumed in our homology modeling studies that the catalytic triad of ABHD6 comprises Ser 148–His 306–Asp 278 and the oxyanion hole is formed by Met 149 and Phe 80.[14] A homology model of ABHD6 has been successfully used in docking studies.[31] Our comparative modeling studies suggested that among the current template structures available, template PDB ID: 2XMZ[32] resulted in optimal active site geometry for docking studies.

The docking poses of highest affinity support the idea that bulkiness at the main core and leaving group modulate the selectivity for ABHD6 over FAAH. In the case of ABHD6, compounds **54** and **55** (JZP-430), which have larger cyclic rings at the main core, have a complementary shape with the active site cavity of our model (Figure 7). In addition, the piperidine/morpholine rings dock well to the other end of the L-shaped site. However, the *N*-containing bicyclic rings of compounds **29** and **30** seem to be too rigid and thus failed to dock at this position. As a consequence, modeling studies suggest that good inhibitory activity is gained when proper shape complementarity meets easy access for the carbonyl to oxyanion hole prior to nucleophilic attack. Compounds **54** and **55** (JZP-430) have more spacious aliphatic ring structures located in this narrower region of the FAAH active site, so no converged docking poses were found. When examining the interaction of compounds **29** and **30** with FAAH, the bulkiest *N*-containing bicyclic ring system was found to dock to the entrances of the acyl binding site and membrane access channel, while the piperidine/morpholine rings fit well in the mouth of the cytoplasm exit (Figure S5, Supporting Information).

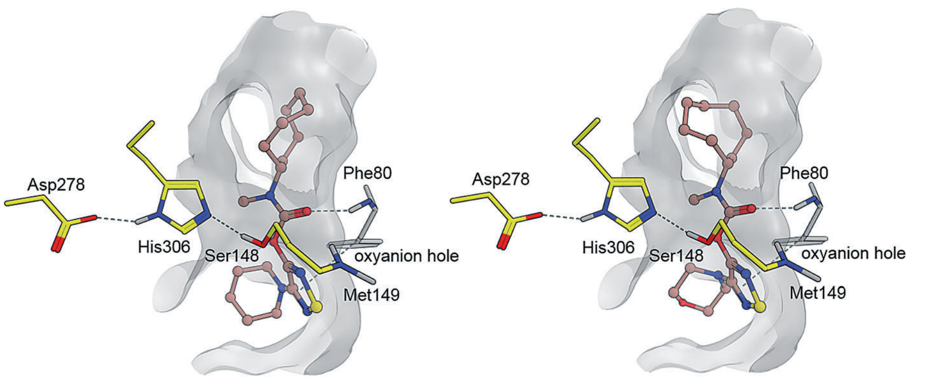

Figure 7. Most favorable Glide docking poses of high-affinity compounds **54** (left) and **55** (JZP-430) (right) to the ABHD6 active site in a homology model. Catalytic residues are colored using yellow carbon atoms, and the surface of the active site is presented.

Conclusions

In this study, we identified 1,2,5-thiadiazole carbamates as novel ABHD6 inhibitors and used molecular modeling to define their interactions with the catalytic site of the enzyme. The best compound of the series, in terms of both potency and selectivity, was 4-morpholino-1,2,5-thiadiazol-3-yl cyclooctyl(methyl)carbamate (JZP-430, **55**), as this compound inhibited human α/β hydrolase domain 6 with low-nanomolar potency (IC_{50} 44 nM) and was >200-fold selective for ABHD6 over FAAH and LAL enzymes. Moreover, compound **55** showed good selectivity for ABHD6 over the other serine hydrolases detected in the mouse brain membrane proteome using ABPP. Compound **55** (JZP-430) showed irreversible binding in our reversibility assays and in molecular modeling studies, it was docked well into the active site of hABHD6 and was shown to have favorable interactions, including impor-

© 0000 Wiley-VCH Verlag GmbH & Co. KGaA, Weinheim

tant hydrogen bonding of the carbonyl oxygen atom, to the oxyanion hole.

Experimental Section

Chemistry

Materials and methods: Reagents and solvents were purchased from commercial suppliers and were used without further purification. Reactions were monitored by thin-layer chromatography using aluminum sheets coated with silica gel F_{245} (60 Å, 40–63 μm, 230–400 mesh) with suitable UV visualization. Purification was carried out by flash chromatography (FC) on J. T. Baker's silica gel for chromatography (pore size 60 Å, particle size 50 nm). Petroleum ether (PE) used for chromatography is of fraction 40–60 °C. ^{1}H NMR and ^{13}C NMR were recorded on a Bruker Avance AV 500 (Bruker Biospin, Switzerland) spectrometer operating on 500.1 and 125.8 MHz, respectively. Tetramethylsilane (TMS) was used as an internal standard for ^{1}H NMR. Chemical shifts are reported in ppm on the δ scale from an internal standard of solvent ($CDCl_3$ 7.26 and 77.0 ppm, DMSO 2.50). The spectra were processed from the recorded FID files with TOPSPIN 2.1 software. The following abbreviations are used: s, singlet; br s, broad singlet; d, doublet; t, triplet; q, quartet; m, multiplet. Coupling constants are reported in Hz. ESI-MS spectra were acquired using a LCQ quadrupole ion trap mass spectrometer equipped with an electrospray ionization source (Thermo LTQ, San Jose, CA, USA). Elemental analyses were performed on a ThermoQuest CE instrument (EA 1110 CHNS-O) or a PerkinElmer PE 2400 Series II CHNS-O Analyzer.

General procedures for preparation of 1,2,5-thiadiazole carbamates (22–55):[19] KO*t*Bu (1.3 equiv) was added to a solution of 1,2,5-thiadiazole alcohol (1.0 equiv) in dry THF (0.2 M) at 0 °C. The mixture was stirred at the same temperature for 10–30 min. Carbamoyl chloride (1.0 equiv) was added slowly under inert atmosphere. The reaction mixture was allowed to warm and stirred at 20–25 °C for another 16–24 h. The progress of the reaction was monitored by TLC using 20% EtOAc in PE as a mobile phase. Reaction mixture was diluted with EtOAc. It was washed with H_2O and brine. The organic layer was dried over sodium sulfate, filtered and concentrated under vacuum to afford crude 1,2,5-thiadiazole carbamates which were purified by flash column chromatography using PE/EtOAc (9:1) as an eluent. The desired fractions were collected and solvents were evaporated on a rotatory evaporator to afford 1,2,5-thiadiazole carbamates. The obtained solid 1,2,5-thiadiazole carbamate was stirred in minimum amount of solvent (n-hexane or di-isopropyl ether (DIPE)) for 10–12 min and, filtered and dried. The purity of the synthesized 1,2,5-thiadiazole carbamates (**22**–**55**) were determined through combustion analyses and are ≥95% (see Table S1 and S2, Supporting Information).

4-(Piperidin-1-yl)-1,2,5-thiadiazol-3-yl morpholine-4-carboxylate (22): White solid (270 mg, 56%); ^{1}H NMR ($CDCl_3$): δ = 3.74–3.70 (br s, 4H), 3.66–3.62 (br s, 2H), 3.55–3.51 (br s, 2H), 3.37–3.35 (m, 4H), 1.64–1.60 ppm (m, 6H); ^{13}C NMR ($CDCl_3$): δ = 153.7, 150.9, 146.2, 66.6, 66.4, 49 (2C), 45.2, 44.5, 25.4 (2C), 24.2 ppm; MS (ESI+): *m/z* = 299.05 $[M+H]^+$.

4-Morpholino-1,2,5-thiadiazol-3-yl piperidine-1-carboxylate (23): White solid (190 mg, 42%); ^{1}H NMR ($CDCl_3$): δ = 3.81–3.79 (m, 4H), 3.59–3.57 (m, 2H), 3.54–3.53 (m, 2H), 3.45–3.44 (m, 4H), 1.69–1.57 ppm (m, 6H); ^{13}C NMR ($CDCl_3$): δ = 153.1, 150.8, 146.7, 66.3 (2C), 48.1 (2C), 46, 45.6, 26, 25.4, 24 ppm; MS (ESI+): *m/z* = 299.02 $[M+H]^+$.

4-(Piperidin-1-yl)-1,2,5-thiadiazol-3-yl pyrrolidine-1-carboxylate (24): White solid product (55 mg, 12%); ^{1}H NMR ($CDCl_3$): δ = 3.58–3.55 (m, 2H), 3.53–3.50 (m, 2H), 3.43–3.40 (m, 4H), 2.0–1.93 (m, 4H), 1.67–1.62 ppm (m, 6H); ^{13}C NMR ($CDCl_3$): δ = 153.7, 150.3, 146.6, 49 (2C), 46.8, 46.7, 29.7, 25.8, 25.4, 24.9, 24.2 ppm; MS (ESI+): *m/z* = 283.22 $[M+H]^+$.

4-(Piperidin-1-yl)-1,2,5-thiadiazol-3-yl 3,4-dihydroisoquinoline-2(1*H*)-carboxylate (25): Brown oil (90 mg, 62%); ^{1}H NMR ($CDCl_3$): δ = 7.24–7.10 (m, 4H), 4.79 (s, 1H), 4.71 (s, 1H), 3.87 (t, *J* = 5.6 Hz, 1H), 3.81 (t, *J* = 5.6 Hz, 1H), 3.38–3.35 (m, 4H), 2.95 (t, *J* = 5.9 Hz, 2H), 1.65–1.59 ppm (m, 6H); ^{13}C NMR ($CDCl_3$): δ = 153.7, 151.2, 146.4, 134.6, 132.5, 128.9, 127, 126.7, 126.4, 49, 46.5, 42.6, 38.7, 30, 25.9, 25.4, 24.4 ppm; MS (ESI+): *m/z* = 345.64 $[M+H]^+$.

4-(4-Phenylpiperidin-1-yl)-1,2,5-thiadiazol-3-yl piperidine-1-carboxylate (26): White solid product (542 mg, 42%); ^{1}H NMR ($CDCl_3$): δ = 7.30 (t, *J* = 7.5 Hz, 2H), 7.21 (t, *J* = 8.3, 3H), 4.13–4.07 (m, 2H), 3.57–3.55 (br s, 2H), 3.54–3.50 (br s, 2H), 3.03–2.97 (m, 2H), 2.72–2.68 (m, 1H), 1.92–1.80 (m, 4H), 1.65–1.61 (m, 4H), 1.56–1.52 ppm (m, 2H); ^{13}C NMR ($CDCl_3$): δ = 153.5, 150.8, 146.7, 145.6, 128.5 (2C), 126.7 (2C), 126.4, 48.7 (2C), 45.9, 45.5, 42.4, 32.9, 32.8, 26, 25.4, 24 ppm; MS (ESI+): *m/z* = 373.25 $[M+H]^+$.

4-(4-Phenylpiperazin-1-yl)-1,2,5-thiadiazol-3-yl piperidine-1-carboxylate (27): White solid (63 mg, 8%); ^{1}H NMR ($CDCl_3$): δ = 7.26 (t, *J* = 8.0 Hz, 2H), 6.94 (d, *J* = 7.9 Hz, 2H), 6.88 (t, *J* = 7.3 Hz, 1H), 3.60–3.58 (m, 6H), 3.53–3.49 (br s, 2H), 3.27–3.25 (m, 4H), 1.67–1.63 ppm (br s, 6H); ^{13}C NMR ($CDCl_3$): δ = 153.1, 151.1, 150.8, 147.2, 129.2 (2C), 120.4, 116.5 (2C), 49 (2C), 47.9 (2C), 46, 45.6, 26, 25.4, 24.1 ppm; MS (ESI+): *m/z* = 374.21 $[M+H]^+$.

4-(4-Benzylpiperidin-1-yl)-1,2,5-thiadiazol-3-yl piperidine-1-carboxylate (28): White solid (134 mg, 31%); ^{1}H NMR (DMSO): δ = 7.27 (t, *J* = 7.5 Hz, 2H), 7.17 (t, *J* = 7.0 Hz, 3H), 4.02 (s, 1H), 3.86 (d, *J* = 12.8 Hz, 2H), 3.56–3.51 (br s, 2H), 3.43–3.38 (br s, 2H), 3.32–3.28 (m, 1H), 2.83 (t, *J* = 11.9 Hz, 2H), 2.53–2.51 (m, 2H), 1.75–1.71 (m, 1H), 1.63–1.52 (m, 6H), 1.27–1.19 ppm (m, 2H); ^{13}C NMR ($CDCl_3$): δ = 153.5, 150.8, 146.6, 140.2, 129.1 (2C), 128.3 (2C), 126, 48.3, 46, 45.5, 43.1, 37.8, 31.6 (2C), 29.7, 26, 25.4, 24.1 ppm; MS (ESI+): *m/z* = 387.23 $[M+H]^+$.

4-(3,4-Dihydroisoquinoline-2-(1*H*)-yl)-1,2,5-thiadiazole-3-yl piperidine-1-Carboxylate (29): Off white solid (230 mg, 42%); ^{1}H NMR ($CDCl_3$): δ = 7.18–7.09 (m, 4H), 4.67 (s, 2H), 3.75 (t, *J* = 5.7 Hz, 2H), 3.65–3.61 (br s, 2H) 3.55–3.51 (br s, 2H), 2.96 (t, *J* = 5.9 Hz, 2H), 1.68–1.64 ppm (m, 6H); ^{13}C NMR ($CDCl_3$): δ = 152.8, 150.9, 146.2, 134, 133.4, 128.8, 126.5, 126.3 (2C), 49.7, 46, 45.6, 45.3, 28.7, 26, 25.4, 24.1 ppm; MS (ESI+): *m/z* = 345.19 $[M+H]^+$.

4-(Octahydroisoquinoline-2-(1*H*)-yl)-1,2,5-thiadiazole-3-yl piperidine-1-carboxylate (30): White solid (200 mg, 68%); ^{1}H NMR (DMSO): δ = 3.93–3.90 (br s, 1H), 3.75–3.72 (br s, 1H), 3.54 (d, *J* = 4.8 Hz, 2H), 3.40 (d, *J* = 5.3 Hz, 2H), 2.87 (t, *J* = 12.4 Hz, 1H), 2.54–2.51 (m, 1H), 1.69–1.65 (m, 2H), 1.59–1.48 (m, 9H), 1.25–1.06 (m, 5H), 0.97–0.90 ppm (m, 2H); ^{13}C NMR (CDCl3): δ = 153.5, 150.8, 146.5, 54.3, 48.8, 45.9, 45.5, 41.8, 41.5, 32.9, 32.4, 30.1, 26.3, 26, 25.9, 25.4, 24.1 ppm; MS (ESI+): *m/z* = 351.23 $[M+H]^+$.

4-(Piperidin-1-yl)-1,2,5-thiadiazol-3-yl dimethylcarbamate (31): White solid (220 mg, 79%); ^{1}H NMR ($CDCl_3$): δ = 3.41–3.39 (m, 4H), 3.11 (s, 3H), 3.04 (s, 3H), 1.66–1.62 ppm (m, 6H); ^{13}C NMR ($CDCl_3$): δ = 153.6, 152.1, 146.5, 48.9 (2C), 37, 36.6, 25.3, 25.1, 24.1 ppm; MS (ESI+): *m/z* = 257.04 $[M+H]^+$.

4-(Piperidin-1-yl)-1,2,5-thiadiazol-3-yl methyl(phenyl)carbamate (32): White solid (132 mg, 38%); ^{1}H NMR ($CDCl_3$): δ = 7.42–7.39 (m,

© 0000 Wiley-VCH Verlag GmbH & Co. KGaA, Weinheim

2H), 7.32–7.25 (m, 3H), 3.43–3.38 (brs, 4H), 3.17 (s, 3H), 1.57–1.55 ppm (brs, 6H); ^{13}C NMR (CDCl$_3$): δ=153.4, 151, 146.2, 142, 129.3 (2C), 127.6 (2C), 126.4, 48.8 (2C), 38.7, 25.4, 25.1, 24.2 ppm; MS (ESI+): m/z=319.04 [M+H]$^+$.

4-(Piperidin-1-yl)-1,2,5-thiadiazol-3-yl diphenylcarbamate (33): White solid (273 mg, 88%); ^{1}H NMR (CDCl$_3$): δ=7.38–7.36 (m, 8H), 7.27–7.25 (m, 2H), 3.24–3.20 (brs, 4H), 1.61–1.56 ppm (brs, 6H); ^{13}C NMR (CDCl$_3$): δ=153.6, 150.1, 145.9, 141.4 (2C), 129.2 (8C), 127 (2C), 48.9, 48.7, 25.5, 25.3, 24.1 ppm; MS (ESI+): m/z=381.03 [M+H]$^+$.

4-(Piperidin-1-yl)-1,2,5-thiadiazol-3-yl diisopropylcarbamate (34): Brown oil (627 mg, 36%); ^{1}H NMR (CDCl$_3$): δ=4.63–4.12 (brs, 1H), 3.93–3.91 (brs, 1H), 3.40 (t, J=5.3 Hz 4H), 1.68–1.59 (m, 6H), 1.33–1.29 ppm (m, 12H); ^{13}C NMR (CDCl$_3$): δ=153.9, 150.4, 146.5, 48.7 (2C), 47.2, 46.8, 25.1 (4C), 24, 21.1, 20.1 ppm; MS (ESI+): m/z=313.63 [M+H]$^+$.

4-(Piperidin-1-yl)-1,2,5-thiadiazole-3-yl ethyl(phenyl)carbamate (35): White solid (160 mg, 18%); ^{1}H NMR (CDCl$_3$): δ=7.43–7.27 (m, 5H), 3.83–3.78 (brs, 2H), 3.18–3.15 (brs, 4H), 1.56–1.52 (brs, 6H), 1.25–1.16 ppm (m, 3H); ^{13}C NMR (CDCl$_3$): δ=153.4, 150.5, 146.2, 140.3, 129.3, 129.1, 127.8, 127.6, 48.8, 46.2, 25.5, 25.4 (2C), 24.8, 24.1, 13 ppm; MS (ESI+): m/z=333.06 [M+H]$^+$.

4-(Piperidin-1-yl)-1,2,5-thiadiazol-3-yl benzyl(methyl)carbamate (36): White solid (450 mg, 35%); ^{1}H NMR (CDCl$_3$): δ=7.38–7.26 (m, 5H), 4.61 (d, J=2.7 Hz, 1H), 4.56 (d, J=2.9 Hz, 1H) 3.40–3.32 (m, 4H), 3.30 (s, 3H), 1.58–1.54 ppm (m, 6H); ^{13}C NMR (CDCl$_3$): δ=153.8, 152.2, 146.5, 136.2, 128.8, 127.9, 127.8, 127.1, 53.2, 49, 35.2, 34.2, 29.7, 25.3 (2C), 24.2 ppm; MS (ESI+): m/z=333.08 [M+H]$^+$.

4-(Piperidin-1-yl)-1,2,5-thiadiazol-3-yl methyl(4-nitrophenyl)carbamate (37): White solid (410 g, 70%); ^{1}H NMR (CDCl$_3$): δ=8.28 (d, J=8.95 Hz, 2H), 7.56 (d, J=8.81 Hz, 2H), 3.52 (s, 3H), 3.31–3.26 (brs, 4H), 1.62–1.57 ppm (brs, 6H); ^{13}C NMR (CDCl$_3$): δ=153.5, 150.5, 147.6, 145.6, 144.5, 126.4, 125.9 (2C), 124.6 (2C), 49 (2C), 38.1, 25.5, 25.3, 24 ppm; MS (ESI+): m/z=364.03 [M+H]$^+$.

4-(Piperidin-1-yl)-1,2,5-thiadiazol-3-yl methyl(3-nitrophenyl)carbamate (38): Yellow solid (406 mg, 52%); ^{1}H NMR (CDCl$_3$): δ=8.25–8.19 (m, 2H), 7.77–7.62 (m, 2H), 3.54–3.50 (brs, 4H), 3.28 (s, 3H), 1.62–1.57 ppm (brs, 6H); ^{13}C NMR (CDCl$_3$): δ=153.5, 150.7, 148.7, 145.7, 143.1, 132.3, 130.1, 122.2, 121.3, 49.3, 49, 38.4, 25.5, 25.3, 24.1 ppm; MS (ESI+): m/z=364.04 [M+H]$^+$.

4-(Piperidin-1-yl)-1,2,5-thiadiazol-3-yl methyl(2-nitrophenyl)carbamate (39): Brown oil (1.3 g, 66%); ^{1}H NMR (CDCl$_3$): δ=8.11–8.04 (m, 1H), 7.73–7.68 (m, 1H), 7.57–7.49 (m, 2H), 3.38 (s, 3H), 3.19–3.15 (brs, 4H), 1.55–1.50 ppm (brs, 6H); ^{13}C NMR (CDCl$_3$): δ=153.4, 150.5, 145.6, 134.6, 130.5, 129.4, 128.9, 125.8, 125.7, 48.8 (2C), 38.4, 25.3 (2C), 24.1 ppm; MS (ESI+): m/z=364.05 [M+H]$^+$.

4-(Piperidin-1-yl)-1,2,5-thiadiazol-3-yl (4-cyanophenyl)(methyl)carbamate (40): White solid (333 mg, 60%); ^{1}H NMR (CDCl$_3$): δ=7.71 (d, J=8.65 Hz, 2H), 7.50 (d, J=8.95 Hz, 2H), 3.48 (s, 3H), 3.29–3.24 (brs, 4H), 1.62–1.57 ppm (brs, 6H); ^{13}C NMR (CDCl$_3$): δ=153.5, 150.5, 145.9, 145.6, 133.2, 126.2, 118, 110.8, 49 (2C), 38, 25.3, 25.1, 24 ppm; MS (ESI+): m/z=344.05 [M+H]$^+$.

4-(Piperidin-1-yl)-1,2,5-thiadiazol-3-yl (4-chlorophenyl)(methyl)carbamate (41): White solid (290 mg, 51%); ^{1}H NMR (CDCl$_3$): δ=7.38–7.26 (m, 4H), 3.41–3.37 (m, 4H), 3.20 (s, 3H), 1.60–1.57 ppm (m, 6H); ^{13}C NMR (CDCl$_3$): δ=153.5, 150.8, 146, 140.5, 133.4, 129.5 (2C), 127.8, 126.3, 49.7, 48.9, 38.6, 25.5 (2C), 24.1 ppm; MS (ESI+): m/z=353.03 [M+H]$^+$.

4-(Piperidin-1-yl)-1,2,5-thiadiazol-3-yl (4-fluorophenyl)(methyl)carbamate (42): White solid (250 mg, 46%); ^{1}H NMR (CDCl$_3$): δ=7.30–7.01 (m, 4H), 3.42–3.36 (m, 4H), 3.24–3.17 (m, 3H), 1.63–1.55 ppm (m, 6H); ^{13}C NMR (CDCl$_3$): δ=162.6, 160.6, 153.4, 151, 146.1, 138, 128.3, 127, 116.4, 48.9, 38.9, 29.7, 25.4, 25.3, 24.1 ppm; MS (ESI+): m/z=337.12 [M+H]$^+$.

4-(Piperidin-1-yl)-1,2,5-thiadiazol-3-yl (3-fluorophenyl)(methyl)carbamate (43): White solid (500 mg, 50%); ^{1}H NMR (CDCl$_3$): δ=7.39–7.36 (m, 1H), 7.15–7.02 (m, 3H), 3.42 (s, 3H), 3.26–3.22 (m, 4H), 1.59–1.55 ppm (m, 6H); ^{13}C NMR (CDCl$_3$): δ=163.7, 161.8, 153.5, 150.8, 147, 143.5, 130.5 (3C), 49 (2C), 29.7, 25.4 (2C), 24.2 ppm; MS (ESI+): m/z=337.12 [M+H]$^+$.

4-(Piperidin-1-yl)-1,2,5-thiadiazol-3-yl methyl(*p*-tolyl)carbamate (44): White solid (110 mg, 20%); ^{1}H NMR (CDCl$_3$): δ=7.28–7.19 (m, 4H), 3.39–3.35 (m, 4H), 3.19 (s, 3H), 2.38 (s, 3H), 1.62–1.55 ppm (m, 6H); ^{13}C NMR (CDCl$_3$): δ=153.5, 151.1, 146.3, 139.4, 137.6, 130, 126.2, 49.2, 48.8 (2C), 38.8, 25.6, 25.4 (2C), 24.1, 21 ppm; MS (ESI+): m/z=333.06 [M+H]$^+$.

4-(Piperidin-1-yl)-1,2,5-thiadiazol-3-yl methyl(*m*-tolyl)carbamate (45): Colorless oil (290 mg, 40%); ^{1}H NMR (CDCl$_3$): δ=7.27 (d, J=7.17 Hz, 1H), 7.15–7.10 (brs, 3H), 3.40–3.35 (brs, 3H), 3.23–3.17 (brs, 4H), 2.39–2.34 (s, 3H), 1.58–1.53 ppm (brs, 6H); ^{13}C NMR (CDCl$_3$): δ=153.6, 151.1, 146.3, 142, 139.5, 129.2, 128.5, 127.2, 123.6, 48.9 (2C), 38.8, 25.5 (2C), 24.2, 21.3 ppm; MS (ESI+): m/z=333.06 [M+H]$^+$.

4-(Piperidin-1-yl)-1,2,5-thiadiazol-3-yl methyl(*o*-tolyl)carbamate (46): White solid (233 mg, 32%); ^{1}H NMR (CDCl$_3$): δ=7.28–7.20 (m, 4H), 3.31 (s, 3H), 3.17–3.14 (brs, 4H), 2.35 (s, 3H), 1.55–1.49 ppm (brs, 6H); ^{13}C NMR (CDCl$_3$): δ=153.4, 151.2, 146.2, 140.6, 135.4, 131.2 (2C), 128.4, 127.1, 49.1, 48.8, 37.7, 25.4 (2C), 24.2, 17.5 ppm; MS (ESI+): m/z=333.08 [M+H]$^+$.

4-(Piperidin-1-yl)-1,2,5-thiadiazol-3-yl (4-methoxyphenyl)(methyl)carbamate (47): White solid (290 mg, 52%); ^{1}H NMR (CDCl$_3$): δ=7.22 (d, J=8.05 Hz, 2H), 6.90 (d, J=8.81 Hz, 2H), 3.81 (s, 3H), 3.35 (s, 3H), 3.22–3.17 (brs, 4H), 1.61–1.58 ppm (brs, 6H); ^{13}C NMR (CDCl$_3$): δ=158.7, 153.4, 151.2, 146.2, 134.7, 127.6, 126.3, 114.4 (2C), 55.4, 48.8 (2C), 39, 25.5, 25.3, 24.1 ppm; MS (ESI+): m/z=349.04 [M+H]$^+$.

4-(Piperidin-1-yl)-1,2,5-thiadiazol-3-yl (3-methoxyphenyl)(methyl)carbamate (48): White solid (600 mg, 80%); ^{1}H NMR (CDCl$_3$): δ=7.34–7.28 (m, 1H), 6.94–6.87 (m, 3H), 3.83 (s, 3H), 3.42 (d, J=8.9 Hz, 7H), 1.71–1.65 ppm (brs, 6H); ^{13}C NMR (CDCl$_3$): δ=160.2, 153.4, 151, 146.1, 143.1, 130 (2C), 118.6, 113, 112.5, 55.4, 48.8, 38.6, 29.6, 25.1, 24.1 ppm; MS (ESI+): m/z=349.07 [M+H]$^+$.

4-(Piperidin-1-yl)-1,2,5-thiadiazol-3-yl (2-methoxyphenyl)(methyl)carbamate (49): White solid (102 mg, 15%); ^{1}H NMR (CDCl$_3$): δ=7.35–7.27 (m, 2H), 6.99–6.97 (m, 2H), 3.88 (s, 3H), 3.31 (s, 3H), 3.26–3.21 (brs, 4H), 1.58–1.52 ppm (brs, 6H); ^{13}C NMR (CDCl$_3$): δ=154.9, 153.2, 151.5, 146.2, 130.5, 129.4, 128.6, 120.8, 112.1, 55.6, 49, 48.6, 37.7, 25.1 (2C), 24.1 ppm; MS (ESI+): m/z=349.01 [M+H]$^+$.

4-(Piperidin-1-yl)-1,2,5-thiadiazol-3-yl [1,1′-biphenyl]-3-yl(methyl)carbamate (50): White solid (280 mg, 60%); ^{1}H NMR (CDCl$_3$): δ=7.57–7.52 (m, 4H), 7.48–7.43 (m, 3H), 7.37 (t, J=7.25 Hz, 1H), 7.32–7.28 (m, 1H), 3.45 (s, 3H), 3.22–3.17 (brs, 4H), 1.51–1.48 ppm (brs, 6H); ^{13}C NMR (CDCl$_3$): δ=153.5, 151, 146.2, 142.8, 142.6, 140, 129.7, 129 (3C), 127.9, 127.1 (2C), 126.4, 125.2, 53.4 (2C), 38, 25.3, 25.1, 24 ppm; MS (ESI+): m/z=395.03 [M+H]$^+$.

4-(Piperidin-1-yl)-1,2,5-thiadiazol-3-yl mesityl(methyl)carbamate (51): White solid (233 mg, 30%); ^{1}H NMR (CDCl$_3$): δ=6.91 (s, 2H),

© 0000 Wiley-VCH Verlag GmbH & Co. KGaA, Weinheim

3.24 (s, 3H), 3.19–3.14 (br s, 4H), 2.29 (d, $J=5.15$ Hz, 9H), 1.58–1.53 ppm (br s, 6H); ^{13}C NMR ($CDCl_3$): $\delta=153.5$, 151.6, 146.4, 137.9, 136.9, 136, 135 (2C), 129.4, 129.3, 49.1, 48.7, 36.3, 25.4 (2C), 24.1, 20.9, 17.5 ppm (2C); MS (ESI+): $m/z=361.06$ $[M+H]^+$.

4-(Piperidin-1-yl)-1,2,5-thiadiazol-3-yl cyclohexyl(methyl)carbamate (52): White solid (118 mg, 19%); ^{1}H NMR ($CDCl_3$): $\delta=4.02$–3.97 (m, 1H), 3.42–3.37 (br s, 4H), 2.95–2.91 (d, 3H, two conformations), 1.87–1.77 (m, 4H), 1.75–1.58 (m, 8H), 1.53–1.33 ppm (m, 4H); ^{13}C NMR ($CDCl_3$): $\delta=153.9$, 151.8, 146.8, 56.3, 49 (2C), 30.7, 29.9, 29.7, 25.7, 25.5, 25.4 (2C), 25.3, 24.2 ppm; MS (ESI+): $m/z=325.06$ $[M+H]^+$.

4-(Piperidin-1-yl)-1,2,5-thiadiazol-3-yl cycloheptyl(methyl)carbamate (53): White solid (175 mg, 22%); ^{1}H NMR ($CDCl_3$): $\delta=4.16$–4.14 (m, 1H), 3.43–3.39 (br s, 4H), 2.96–2.90 (d, 3H, two conformations), 1.91–1.86 (br s, 2H), 1.74–1.66 (m, 12H), 1.57–1.51 ppm (m, 4H); ^{13}C NMR ($CDCl_3$): $\delta=153.9$, 151.5, 146.8, 58.3, 49 (2C), 32.9, 32.3, 31, 29.7, 29.4, 27.5, 25.4, 25.2, 25.1, 24.2 ppm; MS (ESI+): $m/z=339.08$ $[M+H]^+$.

4-(Piperidin-1-yl)-1,2,5-thiadiazol-3-yl cyclooctyl(methyl)carbamate (54): White solid (42 mg, 11%); ^{1}H NMR ($CDCl_3$): $\delta=4.30$–4.26 (m, 1H), 3.44–3.39 (br s, 4H), 2.95–2.89 (d, 3H, two conformations), 1.90–1.72 (m, 6H), 1.69–1.51 ppm (m, 14H); ^{13}C NMR ($CDCl_3$): $\delta=$ 153.9, 151.6, 146.8, 56.9, 49 (2C), 32.1, 31.4, 29.7, 26.3, 26.1, 25.5, 25.4 (2C), 24.9 (2C), 24.2 ppm; MS (ESI+): $m/z=353.09$ $[M+H]^+$.

4-Morpholino-1,2,5-thiadiazol-3-yl cyclooctyl(methyl)carbamate (55): White solid (71 mg, 17%); ^{1}H NMR ($CDCl_3$): $\delta=4.27$–4.22 (m, 1H), 3.81–3.79 (m, 4H), 3.45–3.44 (m, 4H), 2.94–2.89 (d, 3H, two conformations), 1.78–1.70 (m, 6H), 1.67–1.51 ppm (m, 8H); ^{13}C NMR ($CDCl_3$): $\delta=153.2$, 151.5, 146.8, 66.4 (2C), 57.1, 48.2, 48.1, 32.2, 31.4, 29.8, 26.3 (2C), 26, 25, 24.9 ppm; MS (ESI+): $m/z=$ 355.02 $[M+H]^+$.

In vitro assays

Determination of ABHD6 activity and reversibility using a sensitive fluorescent glycerol assay: Glycerol liberated from 1-AG hydrolysis was determined with a sensitive fluorescent glycerol assay using lysates of HEK293 cells expressing hABHD6 as previously described.[14,28] In this approach, glycerol production was coupled via a three-step enzymatic cascade to hydrogen peroxide (H_2O_2) dependent generation of resorufin whose fluorescence (λ_{ex} 530; λ_{em} 590 nm) was kinetically monitored using a Tecan Infinite M200 plate reader (Tecan Group Ltd., Männedorf, Switzerland). Briefly, hABHD6-HEK lysates (99 µL, 0.3 µg protein/well) were pretreated for 30 min with the solvent (DMSO) or the inhibitor (1 µL, four to five different concentrations spanning the range 10^{-9} M to 10^{-5} M), after which 1-AG (100 µL, 12.5 µM final concentration) was added and the reaction kinetically monitored for 90 min. The assays routinely contained 0.5% (*w/v*) BSA (essentially fatty acid free) as a carrier; 1-AG was used instead of 2-AG, as this is the preferred endocannabinoid isomer for hABHD6.[14] The IC_{50} values at time-point 90 min were calculated after nonlinear fitting of the inhibitor dose–response curves. Assay blanks without enzyme were included in each experiment and fluorescence of the assay blank was subtracted before calculation of the final results. Reversibility of compounds to inhibit hABHD6 were tested in 96-well plate format using a 40-fold dilution method previously described for testing reversibility of MAGL inhibitors.[28]

Determination of FAAH activity using anandamide as a substrate: Inhibitory activities of the synthesized compounds were determined using membranes of COS-7 cells expressing hFAAH, essentially as previously described.[33] The assay buffer was 50 mM Tris-HCl (pH 7.4); 1 mM EDTA and the test compounds were dissolved in DMSO (the final DMSO concentration was max 5% *v/v*). The incubations were performed in the presence of 0.5% (*w/v*) BSA (essentially fatty acid free). Protein (55 µL, 1 µg protein per well) was pre-incubated with solvent (DMSO) or the inhibitor (5 µL, five to six different concentrations spanning the range 10^{-9} M to 10^{-4} M) for 10 min at 37 °C (60 µL). At the 10 min time point, 20 µM AEA was added so that its final concentration was 2 µM in 100 µL (containing 10 nM of ^{3}H-AEA having specific activity of 60 Ci mmol^{-1} and concentration of 1 mCi mL^{-1}). The incubations proceeded for 10 min at 37 °C. Ethyl acetate (400 µL) was added at the 20 min time point to stop the enzymatic reaction. Additionally, 100 µL of 50 mM Tris-HCl, pH 7.4; 1 mM EDTA was added. Samples were centrifuged for 4 min at RT 13000 rpm, and aliquots (100 µL) from the aqueous phase containing 1-[^{3}H]ethanolamine were measured for radioactivity by liquid scintillation counting (Wallac 1450 MicroBeta; Wallac Oy, Finland).

Determination of LAL activity using 4-methylumbelliferone oleate as a substrate: LAL activity was determined using a previously described method.[19] Briefly, purified human LAL overexpressed in *Pichia pastoris* (phLAL, 0.01 U mL^{-1}, 105 U mg^{-1}) was mixed with compounds at 10 µM and pre-incubated for 20 min at 37 °C. The reaction was started by addition of 4-methylumbelliferone oleate, which was cleaved by enzymatic activity to 4-methylumbelliferone. The reaction was allowed to proceed for 1 h at 37 °C, and enzymatic activity was quantified by subtracting background fluorescence from all the values, and results were normalized to the DMSO control value.

Activity-based protein profiling (ABPP) of serine hydrolases: Competitive ABPP using mouse whole-brain membranes was conducted to visualize the selectivity of inhibitors toward ABHD6 against other serine hydrolases in brain membrane proteome. We used the active site serine-targeting fluorescent fluorophosphonate probe TAMRA-FP as previously described.[14,28] Briefly, brain membranes (100 µg) were treated for 1 h with DMSO or the selected inhibitors, after which TAMRA-FP labeling was conducted for 1 h at RT (final probe concentration 2 µM). The reaction was quenched by addition of 2× gel loading buffer, after which 10 µg protein was loaded per lane and the proteins were resolved in 10% SDS-PAGE together with molecular weight standards. TAMRA-FP labeling was visualized (λ_{ex} 552; λ_{em} 575 nm) using a fluorescent scanner (FLA-3000 laser fluorescence scanner, Fujifilm, Tokyo, Japan).

Ethics statement: For the ABPP experiments in vitro with native mouse brain membrane proteome, membranes prepared from brain tissue of four-week-old male mice were used. The animals were obtained from the National Laboratory Animal Centre, University of Eastern Finland. The animals were sacrificed using decapitation. Approval for the harvesting of animal tissue was applied, registered and obtained from the local welfare officer of the University of Eastern Finland.

Data analyses: The inhibitor dose–response curves and IC_{50} values derived thereof were calculated from nonlinear regressions using GraphPad Prism 5.0 for Windows (GraphPad Software, San Diego, CA (USA): www.graphpad.com) and Matlab.

Molecular modeling

Molecular modeling was performed using Schrödinger Maestro software package[34] and comparative modeling was done using Accelrys Discovery Studio Client. Structures of small molecules

© 0000 Wiley-VCH Verlag GmbH & Co. KGaA, Weinheim

were prepared using the LigPrep module of Schrödinger suite. X-ray crystal structure for the FAAH (PDB ID: 3QK5)[35] and homology model for ABHD6 were used for docking studies. The homology model of ABHD6 is based on 2XMZ template and the model is based on sequence alignment derived from the default blast search (2XMZ:[32] identity 25%, alignment length 269, *E*-value 1.59373e-12, positive 44%, resolution 1.94 Å). The model was constructed using standard settings of Discovery Studio homology modeling protocol. Side chains of the active site residues were further refined using Prime module of Schrödinger. X-ray structure of the FAAH was pre-processed using the protein preparation wizard of Schrödinger suite in order to optimize the hydrogen bonding network and to remove any possible crystallographic artefacts.[36] Prior to Glide docking studies the grid box was centered using corresponding X-ray ligand as template in the case of FAAH and closest active site residues in the case of ABHD6 model. The Ligand docking was performed using default SP settings of Schrödinger Glide using hydrogen bond constraints to oxyanion hole residues (at least one contact required). Graphical illustrations were generated using Molecular Operating Environment software (MOE, 2013.8).[37]

Supporting information

The Supporting Information contains synthesis and spectroscopic characterization of all intermediates **8**–**21**; elemental analyses for all final compounds **22**–**55**; determination of MAGL activity using 2-AG as a substrate; determination of ABHD12 activity using a previously validated sensitive fluorescent glycerol assay; determination of lipophilicity values for compounds **52**–**55**; determination of LAL inhibitory activity (IC_{50}); TAMRA-FP labeling in mouse brain proteome through competitive ABPP assay; cannabinoid receptor activity; molecular modeling studies, and related references.

Author contributions

All authors contributed equally and gave approval to the final version of the manuscript.

Acknowledgements

*We thank Ms. Minna Glad, Ms. Tiina Koivunen, Ms. Helly Rissanen, Ms. Taija Hukkanen, and Ms. Satu Marttila for their skillful technical assistance. We are grateful to Dr. Hong Du (Indiana University School of Medicine) and Dr. Gregory Grabowski (Synageva BioPharma) for the gift of the LAL enzyme. CSC-Scientific Computing, Ltd. is gratefully acknowledged for software licenses and computational resources. Financial support for this study was provided by the Graduate School of Drug Design, University of East Finland (to J.Z.P.), The Academy of Finland (grants 139140 to T.J.N., 127653 to T.P., and 139620 to J.T.L.), Drug Discovery and Chemical Biology (DDCB) Consortium, Biocenter Finland and the US National Institutes of Health (NIH) (grant R37-DK27083). Part of the research was performed under a Marie Curie Intra-European Fellowship awarded to A.A.K. Some of the calculations were performed under a computational grant from the Interdisciplinary Center for Mathematical and Computational Modeling (ICM), Warsaw, Poland (grant G30-18). For collaborative purposes, we are happy to provide our compound JZP-430 (**55**).*

Keywords: ABHD6 · 2-arachidonoylglycerol · cannabinoids · homology modeling · receptors · 1,2,5-thiadiazole carbamates

[1] J. L. Blankman, G. M. Simon, B. F. Cravatt, *Chem. Biol.* **2007**, *14*, 1347–1356.
[2] J. R. Savinainen, S. M. Saario, J. T. Laitinen, *Acta Physiol.* **2012**, *204*, 267–276.
[3] F. Tchantchou, Y. Zhang, *J. Neurotrauma* **2013**, *30*, 565–579.
[4] M. Alhouayek, J. Masquelier, P. D. Cani, D. M. Lambert, G. G. Muccioli, *Proc. Natl. Acad. Sci. USA* **2013**, *110*, 17558–17563.
[5] G. Thomas, J. L. Betters, C. C. Lord, A. L. Brown, S. Marshall, D. Ferguson, J. Sawyer, M. A. Davis, J. T. Melchior, L. C. Blume, A. C. Howlett, P. T. Ivanova, S. B. Milne, D. S. Myers, I. Mrak, V. Leber, C. Heier, U. Taschler, J. L. Blankman, B. F. Cravatt, R. G. Lee, R. M. Crooke, M. J. Graham, R. Zimmermann, H. A. Brown, J. M. Brown, *Cell Rep.* **2013**, *5*, 508–520.
[6] A. Naydenov, E. Horne, C. Cheah, K. Swinney, K. Hsu, J. Cao, W. Marrs, J. Blankman, S. Tu, A. Cherry, S. Fung, A. Wen, W. Li, M. Saporito, D. Selley, B. Cravatt, J. Oakley, N. Stella, *Neuron* **2014**, *83*, 361–371.
[7] A. H. Lichtman, J. L. Blankman, B. F. Cravatt, *Mol. Pharmacol.* **2010**, *78*, 993–995.
[8] P. K. Chanda, Y. Gao, L. Mark, J. Btesh, B. W. Strassle, P. Lu, M. J. Piesla, M. Zhang, B. Bingham, A. Uveges, D. Kowal, D. Garbe, E. V. Kouranova, R. H. Ring, B. Bates, M. N. Pangalos, J. D. Kennedy, G. T. Whiteside, T. A. Samad, *Mol. Pharmacol.* **2010**, *78*, 996–1003.
[9] J. E. Schlosburg, J. L. Blankman, J. Z. Long, D. K. Nomura, B. Pan, S. G. Kinsey, P. T. Nguyen, D. Ramesh, L. Booker, J. J. Burston, E. A. Thomas, D. E. Selley, L. Sim-Selley, Q. Liu, A. H. Lichtman, B. F. Cravatt, *Nat. Neurosci.* **2010**, *13*, 1113–1119.
[10] T. Fiskerstrand, D. H.-B. Brahim, S. Johansson, A. M'zahem, B. I. Haukanes, N. Drouot, J. Zimmermann, A. J. Cole, C. Vedeler, C. Bredrup, M. Assoum, M. Tazir, T. Klockgether, A. Hamri, V. M. Steen, H. Boman, L. A. Bindoff, M. Koenig, P. M. Knappskog, *Am. J. Hum. Genet.* **2010**, *87*, 410–417.
[11] W. R. Marrs, J. L. Blankman, E. A. Horne, A. Thomazeau, Y. H. Lin, J. Coy, A. L. Bodor, G. G. Muccioli, S. S. Hu, G. Woodruff, S. Fung, M. Lafourcade, J. P. Alexander, J. Z. Long, W. Li, C. Xu, T. Moeller, K. Mackie, O. J. Manzoni, B. F. Cravatt, N. Stella, *Nat. Neurosci.* **2010**, *13*, 951–957.
[12] W. Li, J. L. Blankman, B. F. Cravatt, *J. Am. Chem. Soc.* **2007**, *129*, 9594–9595.
[13] W. R. Marrs, E. A. Horne, S. Ortega-Gutierrez, J. A. Cisneros, C. Xu, Y. H. Lin, G. G. Muccioli, M. Lopez-Rodriguez, N. Stella, *J. Biol. Chem.* **2011**, *286*, 28723–28728.
[14] D. Navia-Paldanius, J. R. Savinainen, J. T. Laitinen, *J. Lipid Res.* **2012**, *53*, 2413–2424.
[15] D. A. Bachovchin, T. Ji, W. Li, G. M. Simon, J. L. Blankman, A. Adibekian, H. Hoover, S. Niessen, B. F. Cravatt, *Proc. Natl. Acad. Sci. USA* **2010**, *107*, 20941–20946, S20941/1-S20941/172.
[16] K. Hsu, K. Tsuboi, A. Adibekian, H. Pugh, K. Masuda, B. F. Cravatt, *Nat. Chem. Biol.* **2012**, *8*, 999–1007.
[17] K. Hsu, K. Tsuboi, J. W. Chang, L. R. Whitby, A. E. Speers, H. Pugh, B. F. Cravatt, *J. Med. Chem.* **2013**, *56*, 8270–8279.
[18] F. J. Janssen, H. Deng, M. P. Baggelaar, M. Allarà, T. van der Wel, H. den Dulk, A. Ligresti, A. C. M. van Esbroeck, R. McGuire, V. Di Marzo, H. S. Overkleeft, M. van der Stelt, *J. Med. Chem.* **2014**, *57*, 6610–6622.
[19] A. I. Rosenbaum, C. C. Cosner, C. J. Mariani, F. R. Maxfield, O. Wiest, P. Helquist, *J. Med. Chem.* **2010**, *53*, 5281–5289.
[20] M. Mor, S. Rivara, A. Lodola, P. V. Plazzi, G. Tarzia, A. Duranti, A. Tontini, G. Piersanti, S. Kathuria, D. Piomelli, *J. Med. Chem.* **2004**, *47*, 4998–5008.
[21] J. Z. Long, X. Jin, A. Adibekian, W. Li, B. F. Cravatt, *J. Med. Chem.* **2010**, *53*, 1830–1842.
[22] J. Chang, M. Niphakis, K. Lum, A. Cognetta III, C. Wang, M. Matthews, S. Niessen, M. Buczynski, L. Parsons, B. Cravatt, *Chem. Biol.* **2012**, *19*, 579–588.
[23] M. J. Niphakis, A. B. Cognetta, J. W. Chang, M. W. Buczynski, L. H. Parsons, F. Byrne, J. J. Burston, V. Chapman, B. F. Cravatt, *ACS Chem. Neurosci.* **2013**, *4*, 1322–1332.
[24] A. Minkkilä, S. M. Saario, T. Nevalainen, *Curr. Top. Med. Chem.* **2010**, *10*, 828–858.

© 0000 Wiley-VCH Verlag GmbH & Co. KGaA, Weinheim

[25] M. Feledziak, D. M. Lambert, J. Marchand-Brynaert, G. G. Muccioli, *Recent Pat. CNS Drug Discovery* **2012**, *7*, 49–70.
[26] C. N. Kapanda, J. H. Poupaert, D. M. Lambert, *Curr. Med. Chem.* **2013**, *20*, 1824–1846.
[27] J. L. Blankman, B. F. Cravatt, *Pharmacol. Rev.* **2013**, *65*, 849–871.
[28] N. Aaltonen, J. R. Savinainen, C. R. Ribas, J. Rönkkö, A. Kuusisto, J. Korhonen, D. Navia-Paldanius, J. Häyrinen, P. Takabe, H. Käsnänen, T. Pantsar, T. Laitinen, M. Lehtonen, S. Pasonen-Seppänen, A. Poso, T. Nevalainen, J. T. Laitinen, *Chem. Biol.* **2013**, *20*, 379–390.
[29] J. Z. Patel, T. Parkkari, T. Laitinen, A. A. Kaczor, S. M. Saario, J. R. Savinainen, D. Navia-Paldanius, M. Cipriano, J. Leppänen, I. O. Koshevoy, A. Poso, C. J. Fowler, J. T. Laitinen, T. Nevalainen, *J. Med. Chem.* **2013**, *56*, 8484–8496.
[30] J. R. Savinainen, M. Yoshino, A. Minkkilä, T. Nevalainen, J. T. Laitinen, *Anal. Biochem.* **2010**, *399*, 132–134.
[31] A. L. Bowman, A. Makriyannis, *Chem. Biol. Drug Des.* **2013**, *81*, 382–388.
[32] A. Dawson, P. K. Fyfe, F. Gillet, W. N. Hunter, *BMC Struct. Biol.* **2011**, *11*, 19.
[33] S. M. Saario, A. Poso, R. O. Juvonen, T. Järvinen, O. Salo-Ahen, *J. Med. Chem.* **2006**, *49*, 4650–4656.
[34] Schrödinger release 2013-3: Maestro ver. 9.6, LigPrep ver. 2.8; Protein Preparation Wizard: Epik ver. 2.6, Impact ver. 6.1, Prime ver. 3.4.; Glide ver. 6.1; Schrödinger LLC, New York, NY (USA), **2013**.
[35] D. J. Gustin, Z. Ma, X. Min, Y. Li, C. Hedberg, C. Guimaraes, A. C. Porter, M. Lindstrom, D. Lester-Zeiner, G. Xu, T. J. Carlson, S. Xiao, C. Meleza, R. Connors, Z. Wang, F. Kayser, *Bioorg. Med. Chem. Lett.* **2011**, *21*, 2492–2496.
[36] Discovery Studio Modeling Environment, release 4.0, Accelrys Software Inc., San Diego, CA (USA), **2013**.
[37] Molecular Operating Environment (MOE), ver. 2013.8, Chemical Computing Group Inc., Montreal, QC (Canada), **2013**.

Received: October 21, 2014
Published online on ■■ ■■, 0000

© 0000 Wiley-VCH Verlag GmbH & Co. KGaA, Weinheim

J. Z. Patel, T. J. Nevalainen, J. R. Savinainen, Y. Adams, T. Laitinen, R. S. Runyon, M. Vaara, S. Ahenkorah, A. A. Kaczor, D. Navia-Paldanius, M. Gynther, N. Aaltonen, A. A. Joharapurkar, M. R. Jain, A. S. Haka, F. R. Maxfield, J. T. Laitinen, T. Parkkari**

■■ – ■■

Optimization of 1,2,5-Thiadiazole Carbamates as Potent and Selective ABHD6 Inhibitors

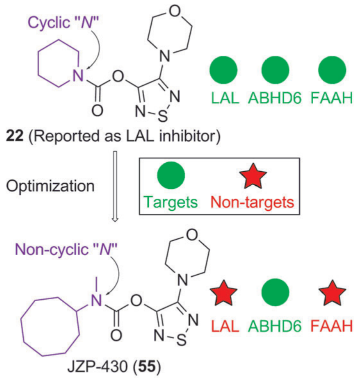

Irreversible and selective: α/β-Hydrolase domain 6 (ABHD6) is an emerging target to treat inflammation, metabolic disorders, and epilepsy. Herein we describe the potent and irreversible inhibition of hABHD6 with 1,2,5-thiadiazole carbamate based compound JZP-430. This compound showed good selectivity over its main supposed off-targets, fatty acid amide hydrolase and lysosomal acid lipase.

© 0000 Wiley-VCH Verlag GmbH & Co. KGaA, Weinheim